Structural Engineering

INTERSECTII
INTERSECTIONS
http://www.ce.tuiasi.ro/intersections

Moment-curvature damage bridge piers subjected horizontal loads

Sergio Oller and Alex H. Barbat

Escuela de Ingenieros de Caminos Canales y Puertos, Universidad Politécnica de Cataluña, Jordi Girona 1-3, C1, 08034 Barcelona, Spain.

Summary

The evaluation of the damage caused by horizontal loads, such as seismic action, to existing bridges has received an important attention in recent years, because it is the first step towards reducing casualties and economic losses. In damage detection and evaluation, the application of simple and reliable models has been prioritized, because they are necessary in further multi-analyses required by Monte Carlo simulations. A simplified moment-curvature damage model, capable of evaluating the expected seismic behaviour of RC highway bridges is proposed in this paper. The damage evaluation model is based on the mechanical modification of the cross sectional inertia of the bridge piers. The model was validated using experimental results obtained at the JRC Ispra for the Warth Bridge of Austria and also FEM analyses performed by other authors for the same bridge.

KEYWORDS: Damage estimation, continuum damage mechanics, damage constitutive model and moment curvature model.

1. INTRODUCTION

Nowadays, the evaluation of the damage caused by earthquakes in existing bridges received great attention. Numerous researches devoted to the structural damage evaluation have been performed, most of them considering the seismic behavior of buildings. The structural damage in the bridges can be characterized in two ways:

1. In the first way, the structural damage is evaluated at given points of the structure by means of local constitutive models describing the damage accumulation caused by a local micro-structural damage [13, 19, 21, 28].
2. In the second way, the local damage is used for the evaluation of global damage indices, which are scalars depending on some variables (or damage parameters) that characterize the dynamic response of the whole system [1, 2, 24].

This paper proposes a damage evaluation based on structural analysis for RC highway bridges with simple pier bents. This typology of bridges was very used all over Europe during the 1960-1980 periods. The proposed structural model is based

ISSN 1582-3024

on the hypothesis of the *flexible pier-rigid deck* behaviour of the structure subjected to seismic loads. A flexible pier-rigid deck simplified model was therefore developed, which could be extending after some modification to other typologies of bridges. This model has been chosen after studying the responses correlation between the proposed model and the real structure [9]. Accordingly, the overall seismic behaviour of this bridge typology is decisively influenced by the damage of the piers. Therefore, the study of the damage produced by horizontal loads has been centered on the piers of the bridge [9], while the structural study of the deck has been performed after the structural analysis of the piers, in an uncoupled way. Thus, the maximum damage of the piers under horizontal loads is the principal aim of the proposed structural damage evaluation procedure.

A local damage index, which describes the state of the material at each point of the structure, is the starting point of the proposed method and is based on a constitutive damage law. Details on this constitutive law are given in the Annex of the paper. The global damage of each pier is obtained form the inertia reduction of the cross sections due to the material degradation. The validation of the proposed model was carried out by using the experimental tests on scale models of the piers of the Warth Bridge, Austria, carried out at the Joint Research Center of Ispra, Italy [25] and a FE model developed by R. Faria [8].

The proposed model permits a simple, reliable and efficient structural analysis. Therefore, it is suitable for considering uncertainties in its parameters and for using Monte Carlo simulations with the aim of evaluating the seismic vulnerability of bridges.

2. STRUCTURAL DESCRIPTION OF THE DYNAMIC MODEL

Reinforced concrete highway bridges with simple pier bents have greater redundancy and higher strength in their longitudinal direction; therefore they will undergo greater damage when subjected to transversal seismic actions. The proposed model aims studying the bridge response to horizontal loads acting transversally to the direction of the bridge axis. Experimental studies confirm that the structural system can be modelled simply by piers loaded transversally to the axis of the bridge interconnected at the deck level by means of box girders [9, 23]. Due to the high stiffness of the bridge in longitudinal direction, the structural analysis in this direction is out of the purposes of this work, focusing on the structural study of the pier in transversal direction.

The model has continuous elements with distributed mass for the piers and concentrated mass for the girders. The motion of the n_p piers in transversal direction to the bridge axis is partially restricted by the adjacent girders that are supported by laminated neoprene bearings. Thus, the displacement of piers causes

Structural Engineering

INTERSECTII
INTERSECTIONS
http://www.ce.tuiasi.ro/intersections

the distortion of the bearings and the consequent rotation of the adjacent girders. The simplified model shown in Figure 1 is based on the following general hypotheses:

1. The piers are continuous elements with distributed mass and infinite axial stiffness.
2. The girders are perfectly stiff elements concentrating the mass at the top of the piers.
3. The bearings of the girders are equivalent short elements that work to shear, having circular cross section and real dimensions.
4. The soil-structure interaction effect on piers and abutments is considered by means of linear springs that represent the rotational stiffness of the soil.
5. The abutments are perfectly stiff.

Accordingly, the model has as many degrees of freedom as transversal displacements at the top of the piers, that is, n_p degrees of freedom.

In following sections, the traverse stiffness of an isolated pier under non lineal damage effects produced by a horizontal load applied at the deck level will be studied.

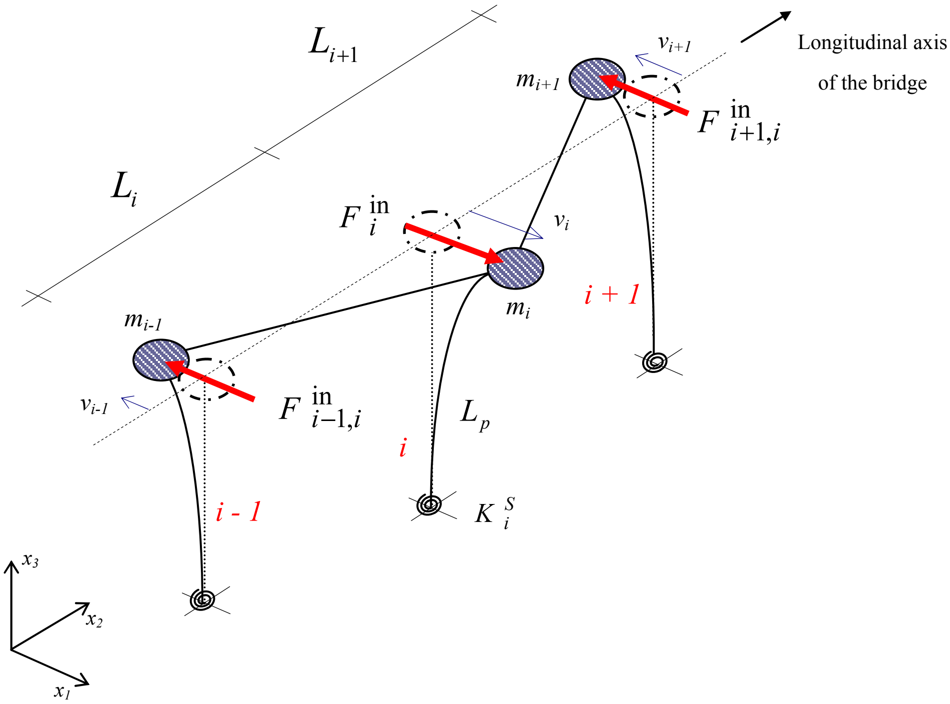

Figure 1. Model for the seismic analysis of the bridge.

ISSN 1582-3024

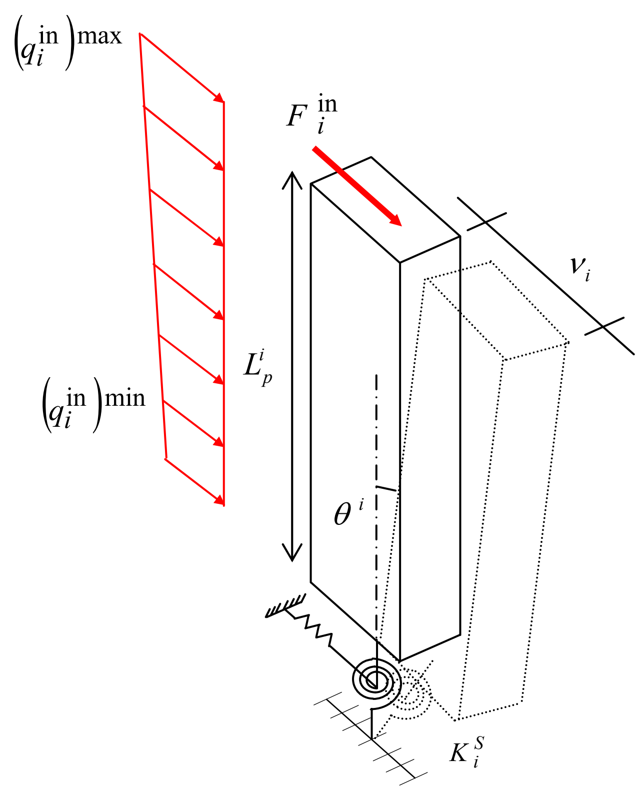

Figure 2. Transversal displacements of pier *I* considering the soil effect.

Transversal behaviour of a single pier

According to the general hypotheses and to Figure 2, the maximum displacement at the top of a pier is

$$v_i = v_\theta^i + v_p^i \tag{1}$$

where

$$v_\theta^i = \theta^i \, L_p^i = \frac{M_i^{max}}{K_i^S} \tag{2}$$

is the elastic displacement produced by a rotation at the base of the pier, and

$$v_p^i = \frac{\left[11\left(q_i^{in}\right)^{max} + 4\left(q_i^{in}\right)^{min}\right]\left(L_p^i\right)^4}{120\, E_{c_i}\, I_i} + \frac{F_i^{in}\left(L_p^i\right)^3}{3\, E_{c_i} I_i} \tag{3}$$

ISSN 1582-3024

Structural Engineering

INTERSECTII
INTERSECTIONS
http://www.ce.tuiasi.ro/intersections

is the elastic displacement produced by external actions [9]. In equations (2) and (3), θ^i is the rotation due to the soil-structure interaction effect, $M_i^{\max}$ is the maximum bending moment at the base of the pier, K_i^S is the equivalent stiffness of the soil, $\left(q_i^{\text{in}}\right)^{\max}$ and $\left(q_i^{\text{in}}\right)^{\min}$ are the maximum and minimum inertial loads by unit length produced by the horizontal acceleration, F_i^{in} is the total inertial force due to the bridge deck and L_p^i, E_{c_i} and I_i are the length, Young's modulus and the inertia of the reinforced concrete cross section of the pier, respectively.

For the maximum displacement of the pier (for $x_3 = 0$), the bending moment equation is [9]

$$M_i(x_3=0) = M_i^{\max} = \frac{\left[2\left(q_i^{\text{in}}\right)^{\max} + \left(q_i^{\text{in}}\right)^{\min}\right]\left(L_p^i\right)^2}{6} + \left(F_i^{\text{in}}\, L_p^i\right) \tag{4}$$

Substituting equations (2), (3) and (4) into Equation (1), the equivalent internal force at the top of the pier is obtained in function of the maximum displacement v_i of the pier [9]

$$F_i^{\text{in}} = \frac{1}{\left[\dfrac{L_p^i}{K_i^S} + \dfrac{\left(L_p^i\right)^3}{3\,E_{c_i}\,I_i}\right]} \times \left[v_i - \frac{\left[2\left(q_i^{\text{in}}\right)^{\max} + \left(q_i^{\text{in}}\right)^{\min}\right]\left(L_p^i\right)^2}{6\,K_i^S} - \frac{\left[11\left(q_i^{\text{in}}\right)^{\max} + 4\left(q_i^{\text{in}}\right)^{\min}\right]\left(L_p^i\right)^4}{120\,E_{c_i}\,I_i}\right] \tag{5}$$

3. NON-LINEAR ANALYSIS OF THE PIER

When the non-linear behavior of the structural materials is taken into account, the undamped equation of motion for each pier is written as

$$m_i\, a_i + F_i^{\text{in}} - \Delta F_i^R = 0 \tag{6}$$

where ΔF_i^R is the residual or out-of-balance force. This unbalanced force is due to the fact that the cross-section inertia and Young modulus are not constant during the non linear process and consequently the solution of Equation (6) should be obtained throughout an iterative process using a non-linear Newmark approach [3, 7].

INTERSECTII
INTERSECTIONS
http://www.ce.tuiasi.ro/intersections

The changes of the pier stiffness and of the internal cross sectional force depend on the damage level reached at each point of the pier whose numerical evaluation is carried out by means of the continuum damage model (see the Annex). In this work, the damage model [19] is used to calculate the local damage index at each point of the structure. Then, by means of a numerical integration of the local damage indices on the cross-section at the base of the piers, the area and the inertia of the damaged cross section are obtained. Obviously, it is possible to obtain the damage evolution at each cross section of the pier, but the moment-curvature model requires the evaluation of damage only at the most loaded section (base cross section).

To obtain the response and the maximum damage of all the bridge piers using the proposed model, Newmark's non-linear algorithm, summarized in Box 1, is used to solve the equilibrium equation at each time of the process. In this analysis the balance force condition is achieved by eliminating $\Delta \mathbf{F}_i^R$ using a Newton-Raphson process. Indirectly, this process also eliminates the residual bending moment $\Delta \mathbf{M} = \mathbf{M}^0 - \mathbf{M}^{\text{int}}$ included in the residual force array, which is the difference between the maximum elastic external moment, $\mathbf{M}^0$, and the pier internal strength capacity moment, $\mathbf{M}^{\text{int}}$. For each step of the non-linear analysis the properties of the system are updated, considering the local degradation of the material caused by the seismic action.

Solution of the dynamic equation of equilibrium

The steps to define the damage in any pier of the bridge are described in boxes 1 and 2. The maximum global damage index of the structure is obtained starting from the cross-sectional damage calculated at the base of the piers for transversal seismic actions. Box 1 shows the numerical procedure to solve the dynamic balance equation (6) using Newmark's non-linear method. As shown previously, the type of bridge under study is modeled by means the piers that behaves like cantilever beams, for which the numerical integration of the damage on the cross section can be simplified, considering in the analysis only the cross-section at the pier base, that is, for $x_3 = 0$. Nevertheless, the procedure could be generalized including when necessary other cross-sections at levels x_3 in the damage integration procedure.

ISSN 1582-3024

1. **Displacement and velocity prediction at** "$t+\Delta t$", starting from null initial conditions

$$\ddot{\tilde{\mathbf{U}}}^{t+\Delta t}=0\ ;\ \dot{\tilde{\mathbf{U}}}^{t+\Delta t}=\dot{\mathbf{U}}^{t}+(1-\gamma)\,\ddot{\mathbf{U}}^{t}\,\Delta t\ ;$$
$$\tilde{\mathbf{U}}^{t+\Delta t}=\mathbf{U}^{t}+\dot{\mathbf{U}}^{t}\,\Delta t+(\tfrac{1}{2}-\beta)\,\ddot{\mathbf{U}}^{t}\,\Delta t^{2}\quad;\quad {}^{i}\Delta\mathbf{f}^{t+\Delta t}=\mathbf{F}_{i}^{q}$$

2. **Computation of displacement increment** $\Delta\mathbf{U}^{t+\Delta t}$ at instant $t+\Delta t$, starting from the linearized balance equation

$${}^{i}\Delta\mathbf{f}^{t+\Delta t}={}^{i}\mathbf{J}^{t+\Delta t}\ {}^{i+1}\Delta\ddot{\mathbf{U}}^{t+\Delta t}\qquad;\qquad {}^{i}\mathbf{J}^{t+\Delta t}={}^{i}\left[\mathbf{M}\cdot\left(\frac{1}{\beta\,\Delta t^{2}}\right)+\mathbf{K}\right]^{t+\Delta t}$$

3. **Displacement** and **velocity correction**

$${}^{i+1}\ddot{\mathbf{U}}^{t+\Delta t}=\left(\frac{1}{\beta\,\Delta t^{2}}\right){}^{i+1}\Delta\ddot{\mathbf{U}}^{t+\Delta t};\quad {}^{i+1}\dot{\mathbf{U}}^{t+\Delta t}=\dot{\tilde{\mathbf{U}}}^{t+\Delta t}+\left(\frac{\gamma}{\beta\,\Delta t}\right){}^{i+1}\Delta\mathbf{U}^{t+\Delta t};\quad {}^{i+1}\mathbf{U}^{t+\Delta t}=\tilde{\mathbf{U}}^{t+\Delta t}+{}^{i+1}\Delta\mathbf{U}^{t+\Delta t}$$

4. **Loop over *k* bridge piers**. The damage constitutive equation are computed at each pier *k* and at each cross section (see next section and Box 2 for more details)

   4a. **Computation of the generalized forces (predictor) and the elastic curvatures and axial strain** at each cross section x_3, using the displacement ${}^{i+1}\mathbf{U}^{t+\Delta t}$ at the top of pier *k*

$$M_1^0(x_3)=\frac{\left(L_p^k-x_3\right)}{\dfrac{\left(L_p^k\right)^2}{K_k^S}+\dfrac{\left(L_p^k\right)^3}{3E_{ck}^0\left(I_k(0)\right)_{11}}}\ {}^{i+1}\left[\mathrm{v}_2(L_p^k)\right]_k^{t+\Delta t}\ ;\ M_2^0(x_3)=\frac{\left(L_p^k-x_3\right)}{\dfrac{\left(L_p^k\right)^2}{K_k^S}+\dfrac{\left(L_p^k\right)^3}{3E_{ck}^0\left(I_k(0)\right)_{22}}}\ {}^{i+1}\left[\mathrm{v}_1(L_p^k)\right]_k^{t+\Delta t}$$

$$N^0(x_3)=N^{ap}\ ;\ \left[\hat{\boldsymbol{\sigma}}^0(x_3)\right]_k=\begin{Bmatrix}N^0(x_3)\\ M_1^0(x_3)\\ M_2^0(x_3)\end{Bmatrix}\ ;\ \left[{}^{i+1}\mathbf{U}^{t+\Delta t}(x_3)\right]_k={}^{i+1}\begin{Bmatrix}\left[\mathrm{u}\ (x_3)\right]_k\\ \left[\mathrm{v}_1(x_3)\right]_k\\ \left[\mathrm{v}_2(x_3)\right]_k\end{Bmatrix}^{t+\Delta t}$$

   4b. **Computation of the residual flexural moment**

For the first load step : $\left[\mathbf{J}(x_3)\right]_k\equiv\left[\mathbf{J}^0(x_3)\right]_k\quad;\quad\left[\hat{\boldsymbol{\sigma}}^{\mathrm{int}}(x_3)\right]_k=\mathbf{0}$

$$\left[\Delta\hat{\boldsymbol{\sigma}}(x_3)\right]_k=\left[\hat{\boldsymbol{\sigma}}^0(x_3)-\hat{\boldsymbol{\sigma}}^{\mathrm{int}}(x_3)\right]_k\ \overset{\text{Unbalanced equivalent force}}{=}\ \left[{}^{i+1}\Delta\mathbf{f}^{t+\Delta t}(x_3)\right]_k=\begin{Bmatrix}{}^{i+1}\Delta N^{t+\Delta t}(x_3)\\ {}^{i+1}\Delta M_1^{t+\Delta t}(x_3)/L_p^k\\ {}^{i+1}\Delta M_2^{t+\Delta t}(x_3)/L_p^k\end{Bmatrix}_k$$

   4c. **Balance equation verification** on the clamped cross section

$$\left\|\Delta\hat{\boldsymbol{\sigma}}(0)\right\|\overset{?}{=}\begin{cases}0 & \Rightarrow\ \text{go to }\textbf{EXIT}\\ \neq 0 & \Rightarrow\ \text{Continue}\end{cases}$$

   4d. **Computation of the incremental generalized strains** and theirs current value

$$\left[{}^{n+1}\Delta\hat{\boldsymbol{\varepsilon}}^{t+\Delta t}(0)\right]_k=-\left[{}^{n}\mathbf{J}^{n+1}(0)\right]_k^{-1}\left[{}^{n}\Delta\hat{\boldsymbol{\sigma}}^{t+\Delta t}(0)\right]_k$$
$$\left[{}^{n+1}\hat{\boldsymbol{\varepsilon}}^{t+\Delta t}(0)\right]_k=\left[{}^{n}\hat{\boldsymbol{\varepsilon}}^{t+\Delta t}(0)\right]_k+\left[{}^{n+1}\Delta\hat{\boldsymbol{\varepsilon}}^{t+\Delta t}(0)\right]_k$$

ISSN 1582-3024

Structural Engineering

INTERSECTII

INTERSECTIONS

http://www.ce.tuiasi.ro/intersections

4e. **Damaged inertia computation at the base cross section of pier** k (see Box 2)

5. **Back to point 4b** followed by the minimization of generalized unbalanced force equation.
6. **Calculate the displacement at each point** x_3 **of the pier and EXIT.**

$$\left[{}^{i+1}\mathbf{U}^{t+\Delta t}(x_3)\right]_k = {}^{i+1}\begin{Bmatrix} \left[\mathrm{u}\;(x_3)\right]_k \\ \left[\mathrm{v}_1(x_3)\right]_k \\ \left[\mathrm{v}_2(x_3)\right]_k \end{Bmatrix}^{t+\Delta t} =$$

$$= {}^{i+1}\begin{Bmatrix} \left[\mathrm{u}\;(x_3-\Delta x_3)\right]_k \\ \left[\mathrm{v}_1(x_3-\Delta x_3)\right]_k \\ \left[\mathrm{v}_2(x_3-\Delta x_3)\right]_k \end{Bmatrix}^{t+\Delta t} - {}^{i+1}\begin{Bmatrix} \left[\varepsilon^N(x_3-\Delta x_3)\right]_k\cdot\Delta x_3 \\ \left[\varphi_2(x_3-\Delta x_3)\right]_k\cdot\Delta x_3 \\ \left[\varphi_1(x_3-\Delta x_3)\right]_k\cdot\Delta x_3 \end{Bmatrix}^{t+\Delta t} + {}^{i+1}\begin{Bmatrix} 0 \\ \dfrac{\left[\chi_2(x_3-\Delta x_3)\right]_k}{2}\cdot\Delta x_3^2 \\ \dfrac{\left[\chi_1(x_3-\Delta x_3)\right]_k}{2}\cdot\Delta x_3^2 \end{Bmatrix}^{t+\Delta t}$$

$${}^{i+1}\begin{Bmatrix} \left[\varphi_1(x_3)\right]_k \\ \left[\varphi_2(x_3)\right]_k \end{Bmatrix}^{t+\Delta t} = {}^{i+1}\begin{Bmatrix} \left[\varphi_1(x_3-\Delta x_3)\right]_k \\ \left[\varphi_2(x_3-\Delta x_3)\right]_k \end{Bmatrix}^{t+\Delta t} + {}^{i+1}\begin{Bmatrix} \left[\chi_1(x_3-\Delta x_3)\right]_k\cdot\Delta x_3 \\ \left[\chi_2(x_3-\Delta x_3)\right]_k\cdot\Delta x_3 \end{Bmatrix}^{t+\Delta t}$$

7. **Back to point 2** after the damage evaluation over all the piers and balance equation over the complete bridge $\left\|{}^{i}\Delta\mathbf{f}^{t+\Delta t}\right\| \to 0$ verification.
8. **New time increment and dynamic load application over all the bridge**. Back to point 1.

Box 1. Solution of the non-linear equilibrium equation applied for the bridge using Newmark`s method.

4. STUDY OF THE DAMAGED CROSS SECTION FOR SKEW BENDING

Theoretical aspects

In order to define the inertia and the bending moment of the damaged base cross section of a pier required by the solution of the non linear equation (6) –see Box 1–, the isotropic damage model [19] has been applied (see Annex). In this section, the way of computing the local damage and its contribution to the cross sectional damage of a pier is described for Bernoulli beams subjected to skew bending. For this purpose, the damaged cantilever beam under skew bending of Figure 3 is considered.

Structural Engineering

INTERSECTII
INTERSECTIONS
http://www.ce.tuiasi.ro/intersections

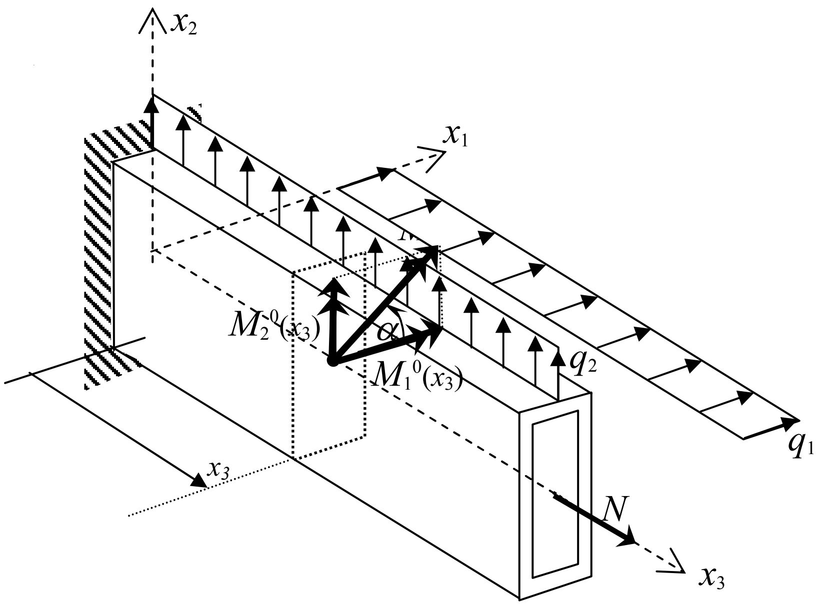

Figure 3. Bridge pier represented as a cantilever Bernoulli beam.

The external loads produce the following generalized forces in a cross section located at a distance x_3

$$\hat{\sigma}^0(x_3) = \begin{Bmatrix} N^0(x_3) \\ M_1^0(x_3) \\ M_2^0(x_3) \end{Bmatrix} = \begin{Bmatrix} N^0(x_3) \\ M^0(x_3)\cdot\cos\alpha \\ M^0(x_3)\cdot\sin\alpha \end{Bmatrix} \tag{7}$$

The following strain and curvature of the Bernoulli beam, due to the elastic bending moment of Equation (7), will be taken as the predictor variables of the algorithm

$$\begin{aligned} \varepsilon^N(x_3) &= \frac{du(x_3)}{dx_3} = \frac{N(x_3)}{E^0\, A^0} \\ \chi_1(x_3) &= -\frac{d^2 v_2(x_3)}{dx_3^2} = \frac{M_1^0(x_3)}{E^o\, I_{11}^0} \\ \chi_2(x_3) &= -\frac{d^2 v_1(x_3)}{dx_3^2} = \frac{M_2^0(x_3)}{E^o\, I_{22}^0} \end{aligned} \tag{8}$$

ISSN 1582-3024

being E^0 the initial undamaged elasticity module, A^0 the initial area of the undamaged cross section and I^0_{ii} the initial inertia of the undamaged of cross section regarding the principal reference system for $x_i \ \forall i = 1,2$.

Considering the Bernoulli beam basic hypotheses, the following expressions for the strain and stress fields are obtained:

$$\begin{cases} \varepsilon(x_1,x_2,x_3) = \varepsilon^N(x_3) + \chi_1(x_3)\cdot x_2 + \chi_2(x_3)\cdot x_1 \\ \qquad = \dfrac{N^0(x_3)}{E^0\,A^0} + \dfrac{M_1^0(x_3)}{E^0 I_{11}^0}x_2 + \dfrac{M_2^0(x_3)}{E^0\,I_{22}^0}x_1 \\ \qquad = \{1 \quad x_2 \quad x_1\}\cdot \begin{bmatrix} E^0\,A^0 & 0 & 0 \\ 0 & E^0\,I_{11}^0 & 0 \\ 0 & 0 & E^0\,I_{22}^0 \end{bmatrix}^{-1} \cdot \begin{Bmatrix} N^0(x_3) \\ M_1^0(x_3) \\ M_2^0(x_3) \end{Bmatrix} \\ \sigma(x_1,x_2,x_3) = E^0\cdot\varepsilon(x_1,x_2,x_3) = \dfrac{N^0(x_3)}{A^0} + \dfrac{M_1^0(x_3)}{I_{11}^0}x_2 + \dfrac{M_2^0(x_3)}{I_{22}^0}x_1 \\ \qquad = \{1 \quad x_2 \quad x_1\}\cdot \begin{bmatrix} A^0 & 0 & 0 \\ 0 & I_{11}^0 & 0 \\ 0 & 0 & I_{22}^0 \end{bmatrix}^{-1} \cdot \begin{Bmatrix} N^0(x_3) \\ M_1^0(x_3) \\ M_2^0(x_3) \end{Bmatrix} \\ \qquad = \mathbf{x}^T\cdot\left[\mathbf{J}^0\right]^{-1}\cdot\hat{\boldsymbol{\sigma}}^0(x_3) \end{cases} \tag{9}$$

All the previous descriptions have been made for a linear elastic skew axial-bending problem. Thus, the material has limitless capacity to resist the applied loads as expressed in Equation (9). This threshold is not possible to be reached for a real material, because its strength is limited to $c^{\max}$, as it can be seen in Equation (A.8) of the Annex. Therefore, the initial generalized internal forces $\hat{\boldsymbol{\sigma}}^0(x_3)$ produced by the external loads $\mathbf{F}^0(x_3)$ is initially unbalanced with the generalized internals stresses $\hat{\boldsymbol{\sigma}}(x_3)$, producing unbalanced residual generalized internal forces $\Delta\hat{\boldsymbol{\sigma}}(x_3)$. These residual stresses should be zero due to the equilibrium condition and this state is reached by increasing the curvature $\Delta\boldsymbol{\chi}(x_3)$ and axial strain $\Delta\varepsilon^N(x_3)$ of the beam. This procedure is iterative and starts with the linearization of the following unbalanced equilibrium equation at each cross section of the beam:

$$\Delta\hat{\boldsymbol{\sigma}}(x_3)=\left[\hat{\boldsymbol{\sigma}}^0(x_3)-\hat{\boldsymbol{\sigma}}^{\text{int}}(x_3)\right]\to\mathbf{0}$$

$$\begin{Bmatrix}\Delta N\ (x_3)\\ \Delta M_1\ (x_3)\\ \Delta M_2(x_3)\end{Bmatrix}=\left[\begin{Bmatrix}N^0(x_3)\\ M_1^0(x_3)\\ M_2^0(x_3)\end{Bmatrix}-\begin{Bmatrix}\int_A\sigma(x_1,x_2,x_3)\cdot dA\\ \int_A\sigma(x_1,x_2,x_3)\cdot x_2\,dA\\ \int_A\sigma(x_1,x_2,x_3)\cdot x_1\,dA\end{Bmatrix}\right]\to\mathbf{0} \tag{10}$$

where the stress at each point of the cross section is obtained by using the constitutive damage model briefly described by the following equations:

$$\begin{aligned}\sigma(x_1,x_2,x_3)&=E(x_1,x_2,x_3)\cdot\varepsilon(x_1,x_2,x_3)\\ &=E(x_1,x_2,x_3)\cdot\left[\varepsilon^N(x_3)+\chi_1(x_3)\cdot x_2+\chi_2(x_3)\cdot x_1\right]\\ \text{with: }\ &E(x_1,x_2,x_3)=f(x_1,x_2,x_3)\cdot E^0\end{aligned} \tag{11}$$

According to the Annex, the evolution of the local damage internal variable at each point of each cross section of the Bernoulli beam, obtained from the local damage constitutive model, is $f(x_1,x_2,x_3)=\left(1-d(x_1,x_2,x_3)\right)=\dfrac{c^{\max}}{c}\,\mathrm{e}^{A\left(1-\frac{c(d)}{c^{\max}}\right)}$, with $0\le c^{\max}\le c$. The values $c^{\max}$ and c are the maximum and current tension strength at each point of the solid, A is a parameter depending of the fracture energy and $E(x_1,x_2,x_3)=f(x_1,x_2,x_3)\cdot E^0$ is the damaged elastic module. Substituting this expression in Equation (10), the residual forces become

$$\begin{aligned}
&\begin{Bmatrix}\Delta N\ (x_3)\\ \Delta M_1\ (x_3)\\ \Delta M_2(x_3)\end{Bmatrix}=\begin{Bmatrix}N^0(x_3)\\ M_1^0(x_3)\\ M_2^0(x_3)\end{Bmatrix}-\begin{Bmatrix}E^0\cdot\int_A f(x_1,x_2,x_3)\cdot\left(\varepsilon^N(x_3)+\chi_1(x_3)\cdot x_2+\chi_2(x_3)\cdot x_1\right)dA\\ E^0\cdot\int_A f(x_1,x_2,x_3)\cdot\left(\varepsilon^N(x_3)\cdot x_2+\chi_1(x_3)\cdot x_2^2+\chi_2(x_3)\cdot x_1\cdot x_2\right)dA\\ E^0\cdot\int_A f(x_1,x_2,x_3)\cdot\left(\varepsilon^N(x_3)\cdot x_1+\chi_1(x_3)\cdot x_2\cdot x_1+\chi_2(x_3)\cdot x_1^2\right)dA\end{Bmatrix}\\
&\begin{Bmatrix}\Delta N\ (x_3)\\ \Delta M_1\ (x_3)\\ \Delta M_2(x_3)\end{Bmatrix}=\begin{Bmatrix}N^0(x_3)\\ M_1^0(x_3)\\ M_2^0(x_3)\end{Bmatrix}-\begin{Bmatrix}E^0\cdot\left(\varepsilon^N(x_3)\cdot A(x_3)+\chi_1(x_3)\cdot m_1(x_3)+\chi_2(x_3)\cdot m_2(x_3)\right)\\ E^0\cdot\left(\varepsilon^N(x_3)\cdot m_1(x_3)+\chi_1(x_3)\cdot I_{11}(x_3)+\chi_2(x_3)\cdot I_{12}(x_3)\right)\\ E^0\cdot\left(\varepsilon^N(x_3)\cdot m_2(x_3)+\chi_1(x_3)\cdot I_{21}(x_3)+\chi_2(x_3)\cdot I_{22}(x_3)\right)\end{Bmatrix}\\
&\begin{Bmatrix}\Delta N\ (x_3)\\ \Delta M_1\ (x_3)\\ \Delta M_2(x_3)\end{Bmatrix}=\begin{Bmatrix}N^0(x_3)\\ M_1^0(x_3)\\ M_2^0(x_3)\end{Bmatrix}-E^0\cdot\begin{bmatrix}A(x_3)&m_1(x_3)&m_2(x_3)\\ m_1(x_3)&I_{11}(x_3)&I_{12}(x_3)\\ m_2(x_3)&I_{21}(x_3)&I_{22}(x_3)\end{bmatrix}\begin{Bmatrix}\varepsilon^N(x_3)\\ \chi_1(x_3)\\ \chi_2(x_3)\end{Bmatrix}\\
&\Delta\hat{\boldsymbol{\sigma}}(x_3)=\hat{\boldsymbol{\sigma}}^0(x_3)-E^0\cdot[\mathbf{J}]\cdot\hat{\boldsymbol{\varepsilon}}(x_3)
\end{aligned} \tag{12}$$

In this equation, $A(x_3)=\int_A f(x_1,x_2,x_3)\cdot dA$ is the damaged cross section, $m_i(x_3)=\int_A f(x_1,x_2,x_3)\cdot x_j\,dA$ are the moment of the damaged area respecting the

INTERSECTII
INTERSECTIONS
http://www.ce.tuiasi.ro/intersections

x_i centroidal principal axes (initially, for undamaged cross section, it is equal to zero), $I_{ii}(x_3)=\int_A f(x_1,x_2,x_3)\cdot x_j^2\,dA$ are the damaged inertia corresponding to the same principal axes x_i and $I_{ij}(x_3)=\int_A f(x_1,x_2,x_3)\cdot\left(x_j\cdot x_i\right)dA$ are the damaged inertia products regarding to the same principal axes (x_i x_j). Notice that the principal inertia axes at certain time instant of the process can change their position in a next instant due to the damage of the cross section of the beam; consequently the damaged inertia products related to the changed axes can be not equal to zero.

Numerical evaluation of the inertia of the damaged cross-section

Due to the difficulties in performing a closed integration of the nonlinear equation (12) using the non-linear damage function defined by Equation (11), the inertia tensor and the area of the damaged cross section is calculated by means of a numerical algorithm (see Box 2). It is important to note that the selected integration algorithm requires to consider that one of the points at which the function to be integrated is located is on the border of the cross section, allowing to capture appropriately the evolution of the damage.

When the cross section of the pier to be analyzed has a rectangular shape, the described procedure is applied directly. However, if the piers have a box shape, the inertia of the damaged cross section is obtained by dividing the element into four subsections, as shown in Figure 4. For each subsection, the damaged area, $A(x_3)_{(\mathrm{J})}$, is

$$A(x_3)_{(\mathrm{J})}=\int_{A_{(\mathrm{J})}} f(x_1,x_2,x_3)\,dA \tag{13}$$

and the distance between the neutral axes of each sub cross section and the global neutral axis of the complete cross section is calculated. The global inertia of the damaged cross section, $\mathbf{I}_T(x_3)_{(\mathrm{J})}$, is then defined by

$$\begin{aligned}\mathbf{I}_T(x_3)_{(\mathrm{J})}&=\sum_{j=1}^{4}\mathbf{I}_{(\mathrm{J})}+A(x_3)_{(\mathrm{J})}\cdot\mathbf{X}^2{}_{(\mathrm{J})}=\\&=\sum_{j=1}^{4}\left\{\begin{bmatrix}\int_{A_{(\mathrm{J})}} f(x_1,x_2,x_3)\cdot x_2^2\,dA & \int_{A_{(\mathrm{J})}} f(x_1,x_2,x_3)\cdot x_2\cdot x_1 dA\\ \int_{A_{(\mathrm{J})}} f(x_1,x_2,x_3)\cdot x_1\cdot x_2\,dA & \int_{A_{(\mathrm{J})}} f(x_1,x_2,x_3)\cdot x_1^2\,dA\end{bmatrix}+\right.\\&\qquad\left.+\left[\int_{A_{(\mathrm{J})}} f(x_1,x_2,x_3)\,dA\right]\cdot\begin{bmatrix}X_{2\,(\mathrm{J})}^2 & X_{2\,(\mathrm{J})}X_{1\,(\mathrm{J})}\\ X_{1\,(\mathrm{J})}X_{2\,(\mathrm{J})} & X_{1\,(\mathrm{J})}^2\end{bmatrix}\right\}\end{aligned} \tag{14}$$

ISSN 1582-3024

where $\mathbf{I}_{(J)}$ is the damaged inertia of subsection j, evaluated by means of Equation (14), $A_{(J)}$ is the damaged area of the subsection j and $\mathbf{X}^2{}_{(J)}$ are the distances between the neutral axis of the subsections and the global neutral axis of the whole cross-section, which depend on the damage at the cross section. In the equations (13) and (14), the numerical integration has been carried out following its classical form

$$
\begin{aligned}
A(x_3)_{(J)} &= \int_{A_{(J)}} f(x_1,x_2,x_3)\cdot dA = J_{acob}\cdot\left[\sum_{p=1}^{n}\sum_{q=1}^{n} w_p\cdot w_q\left[f(\xi_1,\xi_2,x_3)\right]\right]_{(J)} \\
m_i(x_3)_{(J)} &= \int_{A_{(J)}} f(x_1,x_2,x_3)\cdot x_j\, dA \\
&= J_{acob}\cdot\left[\sum_{p=1}^{n}\sum_{q=1}^{n} w_p\cdot w_q\left[f(\xi_1,\xi_2,x_3)\cdot \xi_j\right]\right]_{(J)} \\
I_{ii}(x_3)_{(J)} &= \int_{A_{(J)}} f(x_1,x_2,x_3)\cdot x_j^2\, dA \\
&= J_{acob}\cdot\left[\sum_{p=1}^{n}\sum_{q=1}^{n} w_p\cdot w_q\left[f(\xi_1,\xi_2,x_3)\cdot \xi_j^2\right]\right]_{(J)} \\
I_{ij}(x_3)_{(J)} &= \int_{A_{(J)}} f(x_1,x_2,x_3)\cdot x_j\cdot x_i\, dA \\
&= J_{acob}\cdot\left[\sum_{p=1}^{n}\sum_{q=1}^{n} w_p\cdot w_q\left[f(\xi_1,\xi_2,x_3)\cdot \xi_j\cdot\xi_i\right]\right]_{(J)}
\end{aligned}
\tag{15}
$$

where J_{acob} is the determinant of the gradient of the strains, w_p and w_q are the numerical weight coefficients, ξ_1 and ξ_2 are the isoparametric normalized coordinates and n is the order of the cuadrature of the numerical integration (see Zienkiewicz and Taylor [28]). Particularly, when damage occurs due to the external load, the position of the neutral axis of each subsection is modified according to the area of the subsection that is damaged. This modification must be reflected in the calculation of the distances to the global neutral axis of each subsection. Thus, to obtain each $\mathbf{X}^2{}_{(J)}$, it is necessary to know the coordinates $X_{1\,(J)}$ and $X_{2(J)}$ for each subsection, which are evaluated in a general form by means of the following equations:

ISSN 1582-3024

Structural Engineering

INTERSECTII

INTERSECTIONS

http://www.ce.tuiasi.ro/intersections

$$X_{1\,(\mathrm{J})} = \left[\frac{\int_{A_{(\mathrm{J})}} x_1\, f(x_1,x_2,x_3)\, dA}{\int_{A_{(\mathrm{J})}} f(x_1,x_2,x_3)\, dA} \right]; \quad X_{2\,(\mathrm{J})} = \left[\frac{\int_{A_{(\mathrm{J})}} x_2\, f(x_1,x_2,x_3)\, dA}{\int_{A_{(\mathrm{J})}} f(x_1,x_2,x_3)\, dA} \right] \qquad (16)$$

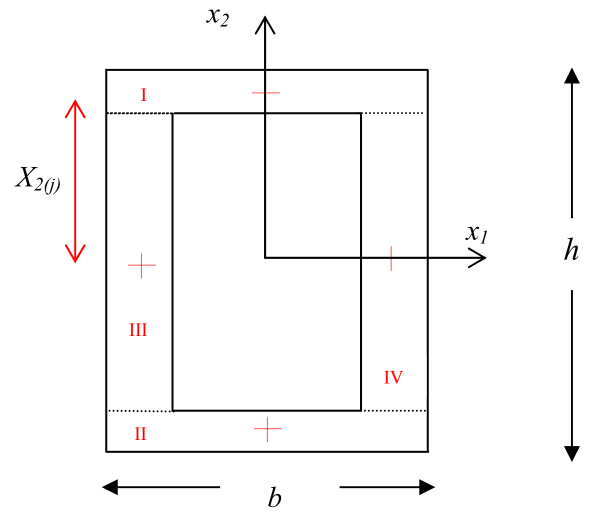

Figure 4. Subsections of a box cross section.

Linearization of the unbalanced equilibrium equation

Linearizing Equation (10) and using the Newton-Raphson procedure, the cross section equilibrium equation is solved by successive iterations, increasing the curvature and axial strain of the pier in the corresponding cross section. For this purpose, the generalized strains (axial strain and bending moment) at increment $(n+1)$ and instant $(t+\Delta t)$ is written by means of Taylor series, truncated at its first term, and then forced to zero

$$\begin{aligned}
\mathbf{0} = {}^{n+1}\Delta\hat{\boldsymbol{\sigma}}^{t+\Delta t}(x_3) &\cong {}^{n}\Delta\hat{\boldsymbol{\sigma}}^{t+\Delta t}(x_3) + \frac{\partial\left[{}^{n}\Delta\hat{\boldsymbol{\sigma}}^{t+\Delta t}(x_3)\right]}{\partial\hat{\boldsymbol{\varepsilon}}} \cdot {}^{n+1}\Delta\hat{\boldsymbol{\varepsilon}}^{t+\Delta t}(x_3) + \ldots \\
&\Rightarrow\ {}^{n+1}\Delta\hat{\boldsymbol{\varepsilon}}^{t+\Delta t}(x_3) = -\left[{}^{n}\mathbf{J}^{n+1}\right]^{-1}\, {}^{n}\Delta\hat{\boldsymbol{\sigma}}^{t+\Delta t}(x_3) \\
&\Rightarrow\ {}^{n+1}\hat{\boldsymbol{\varepsilon}}^{t+\Delta t}(x_3) = {}^{n}\,\hat{\boldsymbol{\varepsilon}}^{t+\Delta t}(x_3) + {}^{n+1}\,\Delta\hat{\boldsymbol{\varepsilon}}^{t+\Delta t}(x_3) \qquad (17) \\
{}^{n+1}\Delta\sigma^{t+\Delta t}(x_1,x_2,x_3) &= E^{0}(x_1,x_2,x_3)\cdot {}^{n+1}\mathbf{x}^{T}\cdot\Delta\hat{\boldsymbol{\varepsilon}}^{t+\Delta t}(x_3) \\
&\Rightarrow\ {}^{n+1}\sigma^{t+\Delta t} = {}^{n}\sigma^{t+\Delta t} + {}^{n+1}\Delta\sigma^{t+\Delta t}
\end{aligned}$$

Structural Engineering

INTERSECTII
INTERSECTIONS
http://www.ce.tuiasi.ro/intersections

being

$$ {}^{n}\mathbf{J}^{n+1} = \frac{\partial\left[{}^{n}\Delta\hat{\boldsymbol{\sigma}}^{t+\Delta t}(x_3)\right]}{\partial\hat{\boldsymbol{\varepsilon}}} = E^0 \cdot \begin{bmatrix} A(x_3) & m_1(x_3) & m_2(x_3) \\ m_1(x_3) & I_{11}(x_3) & I_{12}(x_3) \\ m_2(x_3) & I_{21}(x_3) & I_{22}(x_3) \end{bmatrix} $$

the Jacobian matrix.

For each time increment in which the predictor moment produces an unbalanced load increment greater than an adopted tolerance (equations 17 and 18), the procedure considers an increment of the curvature in order to obtain a corrector of generalized stresses which permits to reach the equilibrium state. The used convergence criterion states that the stable response is obtained for the cross section if

$$ \sqrt{\frac{\sum_i \Delta\hat{\sigma}_i^2}{\sum_i \left(\hat{\sigma}_i^0\right)^2}} \le TOL \tag{18} $$

where TOL is the tolerance adopted ($TOL \rightarrow 0$).

1. Loop over the time $t+\Delta t$

2. Loop over the cross section position x_3

3. Compute the elastic generalized stresses –predictor– for each cross section.

4. Compute the residual generalized internal stresses

For the first load step : $\mathbf{J}(x_3) \equiv \mathbf{J}^0(x_3)$; $\hat{\boldsymbol{\sigma}}^{\text{int}}(x_3) = \mathbf{0}$

$$ \Delta\hat{\boldsymbol{\sigma}}(x_3) = \left[\hat{\boldsymbol{\sigma}}^0(x_3) - \hat{\boldsymbol{\sigma}}^{\text{int}}(x_3)\right] $$

5. Balance equation verification on x_3 cross section :

$$ \left\|\Delta\hat{\boldsymbol{\sigma}}(x_3)\right\| \overset{?}{=} \begin{cases} 0 & \Rightarrow \text{ go to } \textbf{EXIT} \\ \neq 0 & \Rightarrow \text{ Continue} \end{cases} $$

6. Starting loop over Newton-Raphson $n^{\text{iteration}}$ process. Incremental generalized strain computation and obtaining of its current value:

$$ {}^{n+1}\Delta\hat{\boldsymbol{\varepsilon}}^{t+\Delta t}(x_3) = -\left[{}^{n}\mathbf{J}^{n+1}(x_3)\right]^{-1}\, {}^{n}\Delta\hat{\boldsymbol{\sigma}}^{t+\Delta t}(x_3) $$

$$ {}^{n+1}\hat{\boldsymbol{\varepsilon}}^{t+\Delta t}(x_3) = {}^{n}\,\hat{\boldsymbol{\varepsilon}}^{t+\Delta t}(x_3) + {}^{n+1}\,\Delta\hat{\boldsymbol{\varepsilon}}^{t+\Delta t}(x_3) $$

7. Damaged inertia computation at each x_3 cross section of pier k , using the continuum damage model showed in Box A-1 of the Annex:

$$ {}^{n+1}\left[\sigma^{0}\right]^{t+\Delta t}(x_1,x_2,x_3) = E^{0}\cdot{}^{n+1}\mathbf{x}^{T}\cdot{}^{n}\hat{\boldsymbol{\varepsilon}}^{t+\Delta t}(x_3) $$

$$ \mathrm{f}(\sigma^{0}) - {}^{n}\left[c(f)\right]^{t+\Delta t} \begin{cases} \leq 0 & \text{Mantain the inertia value and go to (**)} \\ > & \text{The process of damage continues (*)} \end{cases} $$

$$ (*) \quad {}^{n+1}\left[f(x_1,x_2,x_3)\right]^{t+\Delta t} = \frac{c^{\max}}{c}\ \mathrm{e}^{A\left(1-\frac{c(d)}{c^{\max}}\right)} \quad \text{with} \quad 0 \leq c^{\max} \leq c $$

$$ {}^{n}\mathbf{J}^{t+\Delta t}(x_3) = {}^{n}\begin{bmatrix} \int_A f(x_1,x_2,x_3)\cdot dA & \int_A f(x_1,x_2,x_3)\cdot(x_2)\,dA & \int_A f(x_1,x_2,x_3)\cdot(x_1)\,dA \\ \int_A f(x_1,x_2,x_3)\cdot(x_2)\,dA & \int_A f(x_1,x_2,x_3)\cdot x_2^{2}\,dA & \int_A f(x_1,x_2,x_3)\cdot(x_2\cdot x_1)\,dA \\ \int_A f(x_1,x_2,x_3)\cdot(x_1)\,dA & \int_A f(x_1,x_2,x_3)\cdot(x_1\cdot x_2)\,dA & \int_A f(x_1,x_2,x_3)\cdot x_1^{2}\,dA \end{bmatrix}^{t+\Delta t} $$

$$ (**) \qquad \hat{\boldsymbol{\sigma}}^{\mathrm{int}}(x_3) = E^{0}\cdot{}^{n}\mathbf{J}^{t+\Delta t}(x_3)\cdot{}^{n+1}\hat{\boldsymbol{\varepsilon}}^{t+\Delta t}(x_3) $$

$$ {}^{n+1}\sigma^{t+\Delta t}(x_1,x_2,x_3) = E^{0}(x_1,x_2,x_3)\cdot{}^{n+1}\mathbf{x}^{T}\cdot{}^{n}\hat{\boldsymbol{\varepsilon}}^{t+\Delta t}(x_3) $$

8. Back to point 4
9. **EXIT**

Box 2. Algorithm for the cross sectional damage integration.

5. NUMERICAL EXAMPLE FOR THE WARTH BRIDGE, AUSTRIA

General description of Warth Bridge

The Warth Bridge is located 63 km far from Vienna, Austria, was built 30 years ago and has two spans of the deck of 62.0 m and five of 67.0 m, with a total length of 459.0 m. The seven spans of the bridge give rise to six piers with heights of 31.0 m, 39.0 m, 37.0 m, 36.0 m, 30.0 m and 17.6 m, as it can be observed in Figure 5.

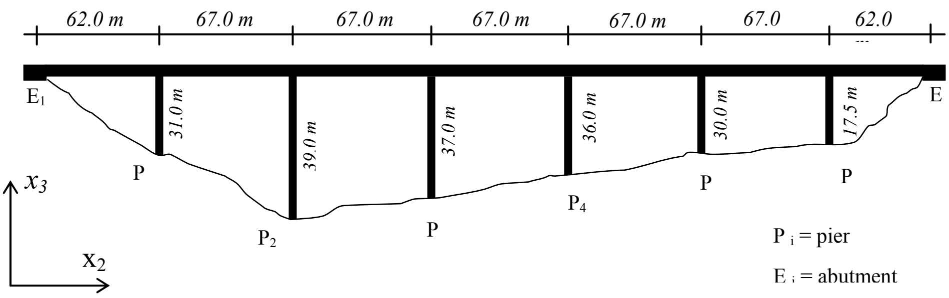

Figure 5. Elevation of the Warth Bridge, Austria.

The geometrical and mechanical properties of the Warth bridge structure were obtained from the original design drawings [25]. Thus, the simple compression strength of the concrete is $f_{cu}^{-} = 45.0\,\mathrm{MPa}$ for girders and $f_{cu}^{-} = 43.0\,\mathrm{MPa}$ for

ISSN 1582-3024

piers. The weight density and Poisson modulus of the concrete are $\gamma = 24.0\ \text{kN/m}^3$ and $\nu = 0.2$, respectively. In order to consider the weight of the non-structural components, the value of the weight density of the girders was increased to a value of $\gamma = 28.0\ \text{kN/m}^3$. For the reinforcement bars, $\gamma = 78.5\ \text{kN/m}^3$, $\nu = 0.3$ and $E_s = 2.0\times10^5$ MPa were considered. The elastic modulus of the reinforced concrete, E_c, was obtained using the Mixing Theory [10, 23] which allows calculating the properties of the elements composed of more than one material.

Quasi static pier response of the Warth Bridge

In this work, the numerical simulation of the quasi static structural behavior of shorter pier of the Warth Bridge is given (identified as P6 in the Figure 5). This pier was studied experimentally in the JCR Ispra Laboratory, Italy [25] and numerically, using a finite elements approach, by Faria et al. [8]. The top of this 5.75 m high pier has been subjected to a horizontal quasi static load. The seismic behavior of the pier has been evaluated using the described Bernoulli beam formulation extended to the non lineal case of Kachanov damage [18, 12]. That is, without using the finite element approach, it has been introduced within the frame of the classical theory of Bernoulli a non lineal continuum damage model. This formulation allows the evaluation of the structural behavior in the non lineal field with a very low computational cost and results comparable with those obtained experimentally and also by means of the finite elements approach are obtained. This model leads to a good, low computational cost, non linear solution required by the evaluation of the seismic vulnerability of the bridge, what implies multiple structural dynamic response calculations. The objective of the structural solution developed in this paper in not only a good prediction of the load-displacement relationship, but also a good evaluation of the cross-sectional damage.

Properties of the materials

The mechanical properties of the reinforced concrete bridge pier are calculated using the mixing theory [4, 23], which combines the mechanical behavior of the concrete and steel. The behavior of the concrete is represented by means of a damage model described in the Annex and the behavior of the steel is represented by means of a anisotropic perfect elasto-plastic model [20]. This combination of the concrete and steel behaviors given by the mixing theory, permits considering a plastic-degradable behavior without softening at each point of the composite material

$$\boldsymbol{\sigma}(d,\boldsymbol{\varepsilon}^p) = k_c\boldsymbol{\sigma}_c(d) + k_s\boldsymbol{\sigma}_s(\boldsymbol{\varepsilon}^p) = \quad k_c\left[(1-d)(\mathbf{C}_0)_c : \boldsymbol{\varepsilon}\right] + k_s\left[(\mathbf{C}_0)_s : (\boldsymbol{\varepsilon} - \boldsymbol{\varepsilon}_s^p)\right] \tag{19}$$

Structural Engineering

INTERSECTII INTERSECTIONS
http://www.ce.tuiasi.ro/intersections

being: $\sigma, \sigma_c(d), \sigma_s(\varepsilon^p)$, the stresses in the composite material, in the damaged concrete and in the plastic steel, respectively. $(\mathrm{C}_0)_c$ and $(\mathrm{C}_0)_s$ are, respectively, the initial constitutive tensors in the concrete and steel while $k_c = A_c(d)/[A_c(d)+A_s]$ and $k_s = A_s/[A_c(d)+A_s]$ are the relative areas corresponding to each material of the cross section of the pier. The characteristics of the used materials are given in Table 1.

Mechanical properties	*Steel*	*Concrete*
Young's modulus	$E_s = 200{,}00\,GPa$	$E_c = 33{,}50\,GPa$
Compression strength at the elastic limit	$f_{sy}^- = 545{,}00 MPa$	$f_{cy}^- = 20{,}00 MPa$
Maximum compression strength	$f_{su}^- = 600{,}00 MPa$	$f_{cu}^- = 43{,}00 MPa$
Tension strength at the elastic limit	$f_{sy}^+ = 545{,}00 MPa$	$f_{cy}^+ = 3{,}10 MPa$
Maximum tension strength	$f_{su}^+ = 600{,}00 MPa$	$f_{cy}^+ = 3{,}10 MPa$
Fracture energy	$(G_f)_s = 12.000{,}00 MN/m$	$(G_f)_s = 1{,}20 MN/m$

Table1. Properties of the materials compounding the reinforced concrete.

The initial values at the clamped cross section, corresponding to the initial, non damaged state, are the following:

$$\begin{gathered}
(A_c)_0 = 0{,}6579\,m^2 \;,\; (A_s)_0 = 76{,}77\times 10^{-4}\,m^2 \Rightarrow \begin{cases} (k_c)_0 = 0{,}9884 \\ (k_s)_0 = 0{,}011533 \end{cases} \\
(E)_0 = (k_c)_0 (E_c)_0 + (k_s)_0 E_s = 35{,}418\,MPa \\
\left.\begin{aligned} (f_y^+)_0 &= (k_c)_0 (f_{cy}^+)_0 + (k_s)_0 (f_{sy}^+)_0 = 9{,}984\,MPa \\ (f_y^-)_0 &= (k_c)_0 (f_{cy}^-)_0 + (k_s)_0 (f_{sy}^-)_0 = 49{,}421\,MPa \end{aligned}\right\} \; n_r = \frac{(f_y^-)_0}{(f_y^+)_0} = 4{,}95
\end{gathered} \tag{20}$$

Geometry and boundary conditions

Figure 6 shows the geometric characteristics and boundary condition for pier P6.

The pier is considered perfectly clamped to the foundation and the following sequence of loads is applied at its upper end:

ISSN 1582-3024

Structural Engineering

INTERSECTII
INTERSECTIONS
http://www.ce.tuiasi.ro/intersections

1. A compressional axial load of 3820,00 kN
2. Once applied this load, three horizontal displacements are applied sequencially
   1) $-0{,}026\,m \le u_h \le +0{,}026\,m$
   2) $-0{,}055\,m \le u_h \le +0{,}055\,m$
   3) $-0{,}1\,m \le u_h \le +0{,}1\,m$

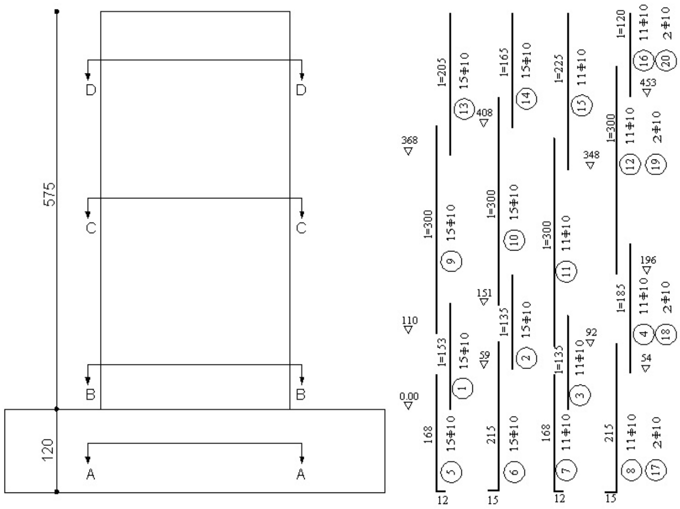

Figure 6. Geometry and reinforcement description of pier P6 belonging to Warth Bridge [25].

These cycles of displacements introduce degradation on the clamped cross section of the pier and the numerical results obtained in this paper (Figure 7.b.) are compared with those obtained by Faria et al. [8] and in the JCR Ispra laboratory [25] (see Figure 7.a).

From the results obtained in the present work by using the damage model and the described structural approach, a good solution is obtained in many cases. In spite of the simplicity of the model, the results, in their general features, reach similar values than those obtained experimentally and numerically through FEM models with two internal damage variables (damage variable for compression and tension). Nevertheless, the most important aspect is the very low computational cost that encourages to its application in solving multiple analysis problems like Monte Carlo simulations [11]. The most important differences between the two graphics of Figure 7 can be observed in the unloading branch, because in this case the recovery of the material properties during the change of the sign of the load is evaluated using a simple constitutive model with a single damage index. In Figure

8 the top pier displacement is represented at the end of the load sequence 1 and then, in the same figure, the deformed pier is drown at the end of the last load sequence 3 In this last case the damaged cross section is localized near the foundation of the pier, while the rest of cross-sections of the pier turns to the its initial un-damaged state (rotation of rigid solid around the kneecap (Figure 8).

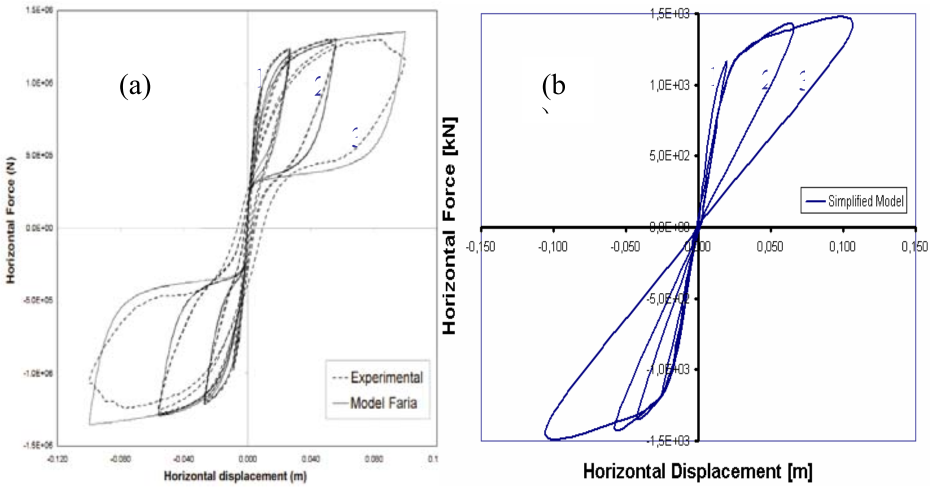

Figure 7. Load-displacement behavior in the pier for the load sequencies 1, 2 and 3. a) Experimental results [25] and numeric results [8]. b) Results obtained in the present work.

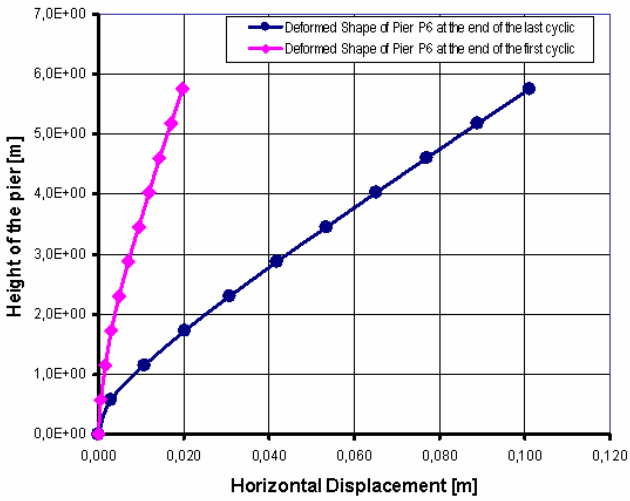

Figure 8. Displacement of the pier P6 at the end of the first load cycle and at the end of the last load cycle.

The degradation of the cross-section is shown in Figure 9. Figure 9a shows the moment-curvature evolution, and Figure 9b shows the evolution of the damage index in function of the curvature. It can be seen in this figure that the level of damage at the end of the process is near to one.

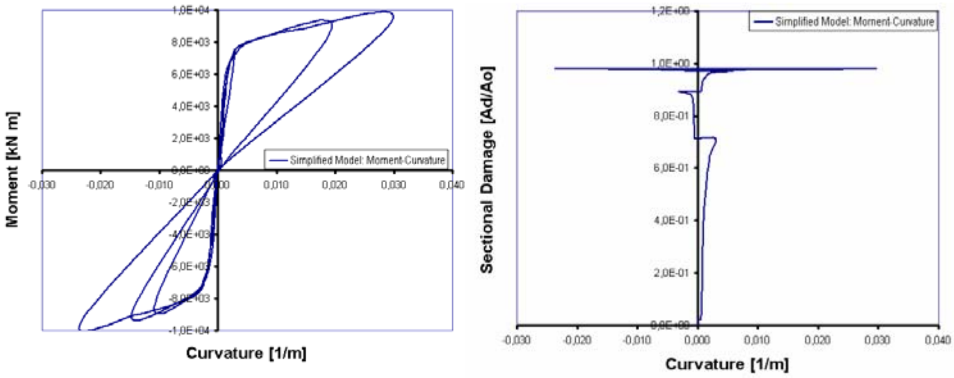

Figure 9. a) Moment-curvature evolution. b) Evolution of the cross-sectional damage depending on the curvature level.

6. SUMMARY AND CONCLUSIONS

A model of evaluation of the damage caused by a horizontal action in the piers of RC bridges with single pier bents is developed in this work. For this structure, the proposed model considers only one degree of freedom for each pier, namely the transversal displacements at their top.

The damage in a pier due to the seismic action is defined by using an isotropic damage model based on the Continuum Damage Mechanics. The damage is obtained in terms of the inertia of the damaged cross section at the base of each bridge pier is obtained. The proposed simplified model was verified using experimental and FEM results.

The simplified non-linear analysis performed with the proposed model gives satisfactory results similar to those of the laboratory test and the FEM results. On the basis of these results it is concluded that the proposed model suitably describes the maximum damages of the piers of RC bridges, and that it is a low-cost computer tool, ideal for the multi-analysis processes required by the evaluation of seismic vulnerability.

A future research objective is to develop a model for the complete bridge, using the developed pier model as an element of the structural model.

ACKNOWLEDGMENTS

This research was partially supported by European Commission Environmental program RTD Project ENV4-CT-97-0574 "Advanced Methods for Assessing the Seismic Vulnerability of Bridges (VAB)", by the Spanish Government (Ministerio de Educación y Ciencia), project REN2002-03365/RIES "Development and application of advanced approaches for the evaluation of the seismic vulnerability and risk of structures (EVASIS)"and project BIA2003-08700-C03-02 "Numerical simulation of the seismic behaviour of structures with energy dissipation devices". This support is gratefully acknowledged.

ANNEX: CONTINUUM CONSTITUTIVE DAMAGE LAW

Introduction to isotropic damage model

This annex contains a brief review of the isotropic continuum damage model at a point of a structure [19], which is used in the paper to formulate the damage of the cross section of a bridge pier. The damage at a point of a continuous solid is defined as the degradation of the stiffness and strength due to the decrease of the effective area [11]. The continuum theory of the damage was formulated by Kachanov [12] in the creep behavior context, but later on it has been reformulated and accepted as a valid alternative to simulate the rate independent behavior of several materials [4-6, 14-17, 26, 27].

Formulation of isotropic damage model

Degradation of the material properties happens due to the presence and growth of small cracks and voids inside the structure of the material. This phenomenon can be simulated by means of the continuum mechanics taking into account a scalar o tensorial internal damage variable. This internal variable of damage measures the level of degradation of the material in a point and its evaluation is based on the transformation of the real stresses in other effective stresses. For the simple isotropic damage used here, the relationship between the real and the effective stress is described using an isotropic damage variable d

$$\boldsymbol{\sigma}_0 = \frac{\boldsymbol{\sigma}}{(1-d)} \tag{A.1}$$

In this equation, d is the internal variable of damage; $\boldsymbol{\sigma}$ it is the Cauchy stress tensor and $\boldsymbol{\sigma}_0$ is the effective stress tensor, evaluated in the "no-damaged" space. This internal variable represents the loss of stiffness level in a point of the material and its upper and lower limits are given by

$$0 \le d \le 1 \tag{A.2}$$

The upper limit (d=1) represents the maximum damage in a point and the lower limit (d=0) represents a non damaged point.

Helmholtz free energy and constitutive equation

The Helmholtz [18] free energy for the isotropic damage model is given by the expression

$$\begin{aligned} \Psi &= \Psi(\boldsymbol{\varepsilon}; p_i) \qquad \text{with} \quad p_i = \{d\} \\ \Psi &= \Psi(\boldsymbol{\varepsilon}; d) = (1-d)\,\Psi_0(\boldsymbol{\varepsilon}) \end{aligned} \tag{A.3}$$

ISSN 1582-3024

The elastic part of the free energy, in the small strain case, can be written in the following quadratic form:

$$\Psi_0(\boldsymbol{\varepsilon}) = \frac{1}{2}\boldsymbol{\varepsilon} : \mathsf{C}_0 : \boldsymbol{\varepsilon} \tag{A.4}$$

where C_0 is the elastic undamaged constitutive tensor. The mechanical part of the dissipation, for uncoupled thermal problem, can be written by using the Clausius-Plank inequality [18]

$$\Xi = \left(\boldsymbol{\sigma} - \frac{\partial \Psi}{\partial \boldsymbol{\varepsilon}}\right) : \dot{\boldsymbol{\varepsilon}} - \frac{\partial \Psi}{\partial d}\dot{d} \geq 0 \tag{A.5}$$

Appling the Coleman method (see Maugin [18]) to the dissipative power (Equation A.5) the following constitutive equation and dissipative inequality are obtained for each point of the material

$$\boldsymbol{\sigma} = \frac{\partial \Psi}{\partial \boldsymbol{\varepsilon}} = (1-d)\frac{\partial \Psi_0}{\partial \boldsymbol{\varepsilon}} = (1-d)\mathsf{C}_0 : \boldsymbol{\varepsilon} \tag{A.6}$$

$$\Xi = \Psi_0 \dot{d} \geq 0 \tag{A.7}$$

Fundamentals of the constitutive damage model

Damage threshold criterion

This approach defines the beginning of the non linear behavior in each point of the solid and it can be defined using the Plasticity Theory

$$\mathsf{F}(\boldsymbol{\sigma}_0;\mathbf{q}) = f(\boldsymbol{\sigma}_0) - c(d) \leq 0, \qquad \text{with} \qquad \mathbf{q} \equiv \{d\} \tag{A.8}$$

where $f(\boldsymbol{\sigma}_0)$ is a scalar function of the stress tensor $\boldsymbol{\sigma}_0 = \mathsf{C}_0 : \boldsymbol{\varepsilon}$ and $c(d)$ is the strength threshold of damage. The initial value of damage is set up on $c(d^0) = c^{\max} = \sigma^{\max}$ and represents the uniaxial strength at crushing state. The damage process begins when $f(\boldsymbol{\sigma}_0)$ is greater than $c^{\max} = \sigma^{\max}$. Equation (A.8) can be written in a more general form throughout the following equivalent expression:

$$\overline{\mathsf{F}}(\boldsymbol{\sigma}_0;\mathbf{q}) = G[f(\boldsymbol{\sigma}_0)] - G[c(d)] \leq 0, \qquad \text{with} \qquad \mathbf{q} \equiv \{d\} \tag{A.9}$$

where $G[\chi]$ is a monotonic scalar function, invertible and positive with positives derivative.

ISSN 1582-3024

Evolution law for the internal damage variable

The evolution law for the internal damage variable can be written in the following general from:

$$\dot{d} = \dot{\mu}\frac{\partial \overline{\mathsf{F}}(\boldsymbol{\sigma}_0;\mathbf{q})}{\partial[f(\boldsymbol{\sigma}_0)]} \equiv \dot{\mu}\frac{\partial G[f(\boldsymbol{\sigma}_0)]}{\partial[f(\boldsymbol{\sigma}_0)]} \tag{A.10}$$

where μ is a non negative scalar value named damage consistency parameter, whose definition is close to the plastic consistency parameter λ. As in the Plasticity Theory, the evaluation of this parameter is made using the Ilyushin [18] consistency condition. From this condition, and from the properties of $G[\chi]$, the following function is obtained:

$$\begin{aligned} &\overline{\mathsf{F}}(\boldsymbol{\sigma}_0;\mathbf{q}) = 0 \;\Rightarrow\; G[f(\boldsymbol{\sigma}_0)] = G[c(d)] \\ &\qquad\Rightarrow\; f(\boldsymbol{\sigma}_0) = c(d) \;\Rightarrow\; \frac{\partial G[f(\boldsymbol{\sigma}_0)]}{\partial f(\boldsymbol{\sigma}_0)} = \frac{\partial G[c(d)]}{\partial c(d)} \end{aligned} \tag{A.11}$$

and, from here, the permanency condition is deduced

$$\begin{aligned} &\dot{\overline{\mathsf{F}}}(\boldsymbol{\sigma}_0;\mathbf{q}) = 0 \quad\Rightarrow\; \frac{\partial G[f(\boldsymbol{\sigma}_0)]}{\partial f(\boldsymbol{\sigma}_0)}\dot{f}(\boldsymbol{\sigma}_0) - \frac{\partial G[c(d)]}{\partial c(d)}\dot{c}(d) = 0 \\ &\qquad\Rightarrow\; \dot{f}(\boldsymbol{\sigma}_0) = \dot{c}(d) \end{aligned} \tag{A.12}$$

Observing the rate of the threshold damage function $\partial G[f(\boldsymbol{\sigma}_0)]/\partial t = \dot{G}[f(\boldsymbol{\sigma}_0)]$ (Equation A.12) and comparing with the evolution law of the internal variable $\dot{d}$ (Equation A.10), the following expression for the damage consistency parameter is obtained:

$$\left.\begin{aligned} &\dot{G}[f(\boldsymbol{\sigma}_0)] = \frac{\partial G[f(\boldsymbol{\sigma}_0)]}{\partial f(\boldsymbol{\sigma}_0)}\dot{f}(\boldsymbol{\sigma}_0) \\ &\dot{d} = \dot{\mu}\frac{\partial G[f(\boldsymbol{\sigma}_0)]}{\partial[f(\boldsymbol{\sigma}_0)]} \end{aligned}\right\} \Rightarrow \begin{aligned} &\dot{d} \equiv \dot{G}[f(\boldsymbol{\sigma}_0)] \;\Rightarrow\; \dot{\mu} \equiv \dot{f}(\boldsymbol{\sigma}_0) = \dot{c}(d) = \\ &= \frac{\partial f(\boldsymbol{\sigma}_0)}{\partial \boldsymbol{\sigma}_0} : \dot{\boldsymbol{\sigma}}_0 = \frac{\partial f(\boldsymbol{\sigma}_0)}{\partial \boldsymbol{\sigma}_0} : \mathsf{C}_0 : \dot{\boldsymbol{\varepsilon}} \end{aligned} \tag{A.13}$$

Time integration over the rate of internal damage variable (Equation A.13) gives the following explicit expression for the damage evaluation in each point of the solid:

$$d = \int_t \dot{d}\; dt = \int_t \dot{G}[f(\boldsymbol{\sigma}_0)]\; dt = G[f(\boldsymbol{\sigma}_0)] \tag{A.14}$$

Substituting Equation (A.14) in (A.5), the following expression for the rate of the mechanical dissipation at each damaged point is established

$$\Xi = \Psi_0\, \dot{G}[f(\boldsymbol{\sigma}_0)] = \Psi_0 \frac{\partial G[f(\boldsymbol{\sigma}_0)]}{\partial f(\boldsymbol{\sigma}_0)} \frac{\partial f(\boldsymbol{\sigma}_0)}{\partial \boldsymbol{\sigma}_0} : \mathsf{C}_0 : \dot{\boldsymbol{\varepsilon}} \qquad \text{(A.15)}$$

The current value for the damage threshold c can be written, at time $s = t$, as

$$c = \max\left\{c^{\max}, \max\left\{f(\boldsymbol{\sigma}_0)\big|_s\right\}\right\} \quad \forall \quad 0 \le s \le t \qquad \text{(A.16)}$$

Particular expression used for the damage threshold criterion

There are several ways to define the damage threshold criterion. In this work, the exponential of reference [19] for concrete structures is used. The scalar function $G[\chi]$ (Equation A.11) is here defined in function of the *unit normalized dissipation variable* κ as [15]

$$\dot{\kappa} = K(\boldsymbol{\sigma}_0)\cdot \Xi_m = \left[\frac{r(\boldsymbol{\sigma}_0)}{g_f} + \frac{1-r(\boldsymbol{\sigma}_0)}{g_C}\right]\cdot \Xi_m \Rightarrow \quad 0 \le \left[\kappa = \int_t \dot{\kappa}\, dt\right] \le 1 \qquad \text{(A.17)}$$

where $\Xi_m = \Psi_0\, \dot{d}$ is the damage dissipation and $r(\boldsymbol{\sigma}) = \sum_{\mathbf{I}=1}^{3} \langle \sigma_{\mathbf{I}} \rangle \Big/ \sum_{\mathbf{I}=1}^{3} |\sigma_{\mathbf{I}}|$ a scalar function to define the sign of the stress state at each point and at each time instant of the damage process, being $\langle x \rangle = 0{,}5\,[x + |x|]$ the McAully function. The variables g_f and g_c are the maximum values for the tension-compression dissipation at each point, respectively [15]. By this way, the damage dissipation will be always normalized to the maximum consumed energy during the mechanical process.

Using κ as an auxiliary variable, it is now possible to evaluate the damage function $G[\chi]$ in the following form [19]:

$$\mathrm{d} = \mathrm{G}[\mathrm{c}(\kappa)] = 1 - \frac{\mathrm{c}^{\max}}{\mathrm{c}(\kappa)}\, \mathrm{e}^{A\left(1 - \frac{\mathrm{c}(\kappa)}{\mathrm{c}^{\max}}\right)} \quad \text{with} \quad 0 \le \mathrm{c}^{\max} \le \mathrm{c}(\mathrm{d}) \qquad \text{(A.18)}$$

but, under the damage condition $f(\boldsymbol{\sigma}_0) \equiv c(\kappa)$. This equation can be also written as

$$G[f(\boldsymbol{\sigma}_0)] = 1 - \frac{f^0(\boldsymbol{\sigma}_0)}{f(\boldsymbol{\sigma}_0)}\, \mathrm{e}^{A\left(1 - \frac{f(\boldsymbol{\sigma}_0)}{f^0(\boldsymbol{\sigma}_0)}\right)} \quad \text{with} \quad f^0(\boldsymbol{\sigma}_0) = c^{\max}$$

ISSN 1582-3024

where $A=\left[g_f/\left(f^0(\boldsymbol{\sigma}_0)\right)^2-0.5\right]^{-1}$ is a parameter depending on the fracture energy dissipation g_f [19]. The value $f^0(\boldsymbol{\sigma}_0)=c^{\max}$ is obtained from the agreement with the first damage threshold, when the condition $G\left[f^0(\boldsymbol{\sigma}_0)\right]-G\left[c^{\max}\right]=0$ is reached and $G\left[f^0(\boldsymbol{\sigma}_0)\right]=G\left[c^{\max}\right]\equiv 0$ shows the damage integration algorithm for each single point of the structure.

1. Compute the elastic prediction stress and the internal variable at current time "$t+\Delta t$", and equilibrium iteration "i", ,

$$[\boldsymbol{\sigma}_0]^{t+\Delta t}=\mathrm{C}_0:[\boldsymbol{\varepsilon}]^{t+\Delta t}$$
$$^i[d]^{t+\Delta t}\;;\;\tau={}^i\left[G[f(\boldsymbol{\sigma}_0)]\right]^{t+\Delta t}$$
$$\tau^0={}^i\left[G\left[f^0(\boldsymbol{\sigma}_0)\right]\right]^{t+\Delta t}$$

2. Damage threshold checking:

a. If: $\tau-\tau^{\max}\le 0$

Then $\left\{\begin{matrix} ^i[\boldsymbol{\sigma}]^{t+\Delta t}=[\boldsymbol{\sigma}_0]^{t+\Delta t} \\ ^i[d]^{t+\Delta t}\;;\;\tau^{\max}=\tau \end{matrix}\right\}$ and go to the **EXIT**

b. If: $\tau-\tau^{\max}>0$

Then start with the damage constitutive integration

3. Integration of the damage constitutive equation,

$$\tau^{\max}=\tau$$
$$^i[d]^{t+\Delta t}=1-{}^i\left[\frac{\tau^0}{\tau}\,\mathrm{e}^{A\left(1-\frac{\tau}{\tau^0}\right)}\right]^{t+\Delta t}$$

4. Stress and tangent constitutive tensor actualization.

$$^i[\boldsymbol{\sigma}]^{t+\Delta t}=(1-{}^i[d]^{t+\Delta t})[\boldsymbol{\sigma}_0]^{t+\Delta t}$$
$$^i\left[\mathrm{C}^T\right]^{t+\Delta t}={}^i\left[(1-d)\mathrm{C}_0-\frac{\partial G[f(\boldsymbol{\sigma}_0)]}{\partial[f(\boldsymbol{\sigma}_0)]}[\mathrm{C}_0:\boldsymbol{\varepsilon}]\otimes\left[\frac{\partial f(\mathrm{C}_0:\boldsymbol{\varepsilon})}{\partial\boldsymbol{\varepsilon}}\right]\right]^{t+\Delta t}$$

5. EXIT

Box A1. Integration of the continuum damage equation at each structural point with exponential softening

ISSN 1582-3024

Stress function particularization

Simo and Ju stress function [26, 27] is used in the paper

$$\tau = f(\boldsymbol{\sigma}_0) = \sqrt{2\,\Psi_0(\boldsymbol{\varepsilon})} = \sqrt{\boldsymbol{\varepsilon} : \mathrm{C}_0 : \boldsymbol{\varepsilon}} \tag{A.19}$$

Taking into account this function, parameter A used in Equation (A.18) can be written as

$$A = \frac{1}{\dfrac{g_f}{\left(f^0(\boldsymbol{\sigma}_0)\right)^2} - \dfrac{1}{2}} \tag{A.20}$$

where g_f represents the maximum of the fracture energy to be dissipated at each point of the solid and $f^0(\boldsymbol{\sigma}_0)$ is the value given by the threshold equation for the first damage threshold.

ISSN 1582-3024

Structural Engineering

INTERSECTII
INTERSECTIONS
http://www.ce.tuiasi.ro/intersections

References

[1] R. Aguiar and A. H. Barbat, "*Daño sísmico en estructuras de hormigón armado*". Universidad Politécnica del Ejercito, Quito, Ecuador., 1997.

[2] S. Arman and M. Grigoriu, *Markov model for local and global damage indexes in seismic analysis,* **NCEER-94-0003**, National Center for Earthquake Engineering Research, 1994.

[3] A. H. Barbat, S. Oller, E. Oñate and A. Hanganu, "Viscous Damage Model for Timoshenko Beam Structures". *International Journal of Solids and Structures*, Vol.34, No.30, pp. 3953-3976. 1997.

[4] E. Car, S. Oller and E. Oñate, "An anisotropic elastoplastic constitutive model for large strain analysis of fiber reinforced composite materials". *Computer Methods in Applied Mechanics and Engineering*, Vol. 185, No. 2-4, 245-277, 2000.

[5] J. Chaboche, "Continuum damage mechanics part I. General Concepts". *Journal of Applied Mechanics*, 55, 59-64, 1988.

[6] J. Chaboche, "Continuum damage mechanics part II. Damage Growth". *Journal of Applied Mechanics,* 55, 65-72, 1988.

[7] R. W. Clough and J. Penzien, *Dynamics of Structures*. McGraw-Hill, 1992.

[8] R. Faria, N. Vila Pouca and R. Delgado, "Simulation of the cyclic behaviour of r/c rectangular hollow section bridge piers via a detailed numerical model". *Journal of Earthquake Engineering*, Vol. 8, No. 5, 725-748, 2004.

[9] C. Gómez-Soberón, S. Oller and A. Barbat, *Seismic vulnerability of bridges using simple models". Monographs of Seismic Engineering*, Monograph series in Earthquake Engineering, **CIMNE IS-47**, International Center of Numerical Methods in Engineering, Barcelona, Spain, 2002.

[10] D. Hull, "*Materiales compuestos",* Reverté Editorial, Spain, 1987.

[11] J. E. Hurtado and A. H. Barbat, "Monte Carlo techniques in computational stochastic mechanics". *Archives of Computational Methods in Engineering*, Vol. 5, No.1, 3-30, 1998.

[12] L. M Kachanov,. "Time of rupture process under creep conditions". *Izvestia Akaademii Nauk; Otd Tech Nauk*, 8 26-31, 1958, .

[13] J. Lemaitre "*A course on damage mechanics*", 2nd edition, Springer, 1992.

[14] J. Lemaitre and J. L. Chaboche "Aspects phénoménologiques de la rupture par endommagement". *Journal of Applied Mechanics*, 2, 317-365, 1978.

[15] J. Lubliner, J. Oliver, S. Oller and E. Oñate, "A plastic damage model for non linear analysis of concrete". *Int. Solids and Structures,* Vol. 25, No. 3, pp. 299-326, 1989.

[16] B. Luccioni and S. Oller, "A directional damage model", *Computer Methods in Applied Mechanics and Engineering*. Vol. 192, No. 9-10, 1119-1145, 2003.

[17] B. Luccioni, S. Oller and R. Danesi, "*Coupled plastic-damaged model". Computer Methods in Applied Mechanics and Engineering*, Vol. 129, No. 1-2, 81-89, 1996.

[18] G. A. Maugin, *The thermomechanics of plasticity and fracture*. Cambridge University Press, 1992.

[19] J. Oliver, M. Cervera, S. Oller and J. Lubliner, "Isotropic damage models and smeared crack analysis of concrete". *Second International Conference on Computer Aided Analysis and Design of Concrete Structures*, **2**, 945-958, Austria, 1990.

[20] S. Oller, E. Car and J. Lubliner, "Definition of a general implicit orthotropic yield criterion". *Computer Methods in Applied Mechanics and Engineering*, Vol. 192, No. 7-8, 895-912, 2003.

[21] S. Oller, B. Luccioni and A. Barbat, "Un método de evaluación del daño sísmico de estructuras de hormigón armado". *Revista Internacional de Métodos Numéricos para el Cálculo y Diseño en Ingeniería*, **12(2)**, 215-238, 1996.

[22] S. Oller, A. H. Barbat, E. Oñate and A. Hanganu, "A damage model for the seismic analysis of buildings structures". *10th World Conference on Earthquake Engineering*. 2593-2598, 1992.
[23] S. Oller, E. Oñate, J. Miquel and S. Botello, "A plastic damage constitutive model for composite material". *International Journal of Solids and Structures*, Vol.33, No.17, pp. 2501-2518, 1996.
[24] Y. J. Park and A. H. Ang, "Mechanistic seismic damage model for reinforced concrete". *Journal of Structural Engineering*, **111(4)**, 722-739, 1985.
[25] A. Pinto, J. Molina and G. Tsionis, *Cyclic Test on a Large Scale Model of an Existing Short Bridge Pier (Warth Bridge-Pier A70)*. EUR Report, Joint Research Centre, ISIS, Ispra, Italy.
[26] J. Simo and J. Ju, "Strain and stress based continuum damage models – I Formulation". *Int. J. Solids Structures*, 23, 821-840, 1987.
[27] J. Simo and J. Ju, "Strain and stress based continuum damage models – II Computational aspects". *Int. J. Solids Structures*, 23, 841-869, 1987.
[28] O. Zienkiewicz and R. Taylor, *The Finite Element Method*. Fourth edition, Volume 1 and 2, McGraw-Hill, 1988.